Title
Nanowire-bacteria hybrids for unassisted solar carbon dioxide fixation to value-added chemicals.

Journal
Nano letters, 15(5)

ISSN
1530-6984

Authors
Liu, Chong
Gallagher, Joseph J
Sakimoto, Kelsey K
et al.

Publication Date
2015-05-01

DOI
10.1021/acs.nanolett.5b01254

Peer reviewed

NANO LETTERS

Letter

pubs.acs.org/NanoLett

Nanowire–Bacteria Hybrids for Unassisted Solar Carbon Dioxide Fixation to Value-Added Chemicals

Chong Liu,[†,⊥] Joseph J. Gallagher,[‡] Kelsey K. Sakimoto,[†] Eva M. Nichols,[†] Christopher J. Chang,*[,†,‡,§,#] Michelle C. Y. Chang,*[,†,‡,#] and Peidong Yang*[,†,⊥,∥,%]

[†]Department of Chemistry, [‡]Department of Molecular and Cell Biology, [§]Howard Hughes Medical Institute, and [∥]Department of Materials Science and Engineering, University of California, Berkeley, Berkeley, California 94720, United States

[⊥]Materials Sciences Division and [#]Chemical Sciences Division, Lawrence Berkeley National Laboratory, Berkeley, California 94720, United States

[%]Kavli Energy NanoSciences Institute, Berkeley, California 94720, United States

Supporting Information

ABSTRACT: Direct solar-powered production of value-added chemicals from CO_2 and H_2O, a process that mimics natural photosynthesis, is of fundamental and practical interest. In natural photosynthesis, CO_2 is first reduced to common biochemical building blocks using solar energy, which are subsequently used for the synthesis of the complex mixture of molecular products that form biomass. Here we report an artificial photosynthetic scheme that functions via a similar two-step process by developing a biocompatible light-capturing nanowire array that enables a direct interface with microbial systems. As a proof of principle, we demonstrate that a hybrid semiconductor nanowire–bacteria system can reduce CO_2 at neutral pH to a wide array of chemical targets, such as fuels, polymers, and complex pharmaceutical precursors, using only solar energy input. The high-surface-area silicon nanowire array harvests light energy to provide reducing equivalents to the anaerobic bacterium, *Sporomusa ovata*, for the photoelectrochemical production of acetic acid under aerobic conditions (21% O_2) with low overpotential (η < 200 mV), high Faradaic efficiency (up to 90%), and long-term stability (up to 200 h). The resulting acetate (~6 g/L) can be activated to acetyl coenzyme A (acetyl-CoA) by genetically engineered *Escherichia coli* and used as a building block for a variety of value-added chemicals, such as *n*-butanol, polyhydroxybutyrate (PHB) polymer, and three different isoprenoid natural products. As such, interfacing biocompatible solid-state nanodevices with living systems provides a starting point for developing a programmable system of chemical synthesis entirely powered by sunlight.

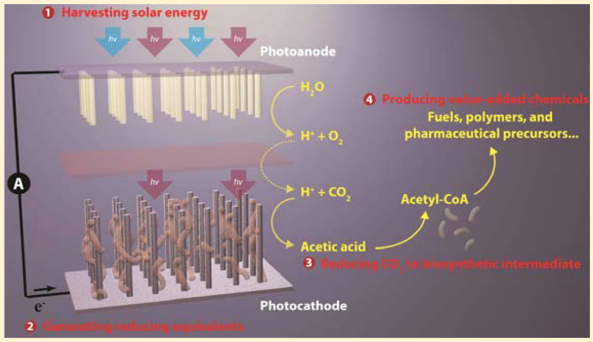

KEYWORDS: *Nanowires, artificial photosynthesis, bacteria, carbon dioxide fixation*

Natural photosynthesis, which harvests 130 TW of solar energy to generate up to 115 billion metric tons of biomass annually from the reduction of CO_2, provides motivation for the development of artificial systems that can capture the energy of the sun to convert CO_2 and H_2O to value-added chemicals of societal benefit.[1−9] However, such an approach has not been fully realized owing to a host of unmet basic scientific challenges.[10] For example, enzymes isolated from microorganisms and plants can selectively catalyze CO_2 reduction with low energy barriers;[11−13] however, they do not self-repair outside their native cellular context and are often intolerant to oxygen. Consequently, bioderived CO_2-reducing catalytic systems are not directly applicable to oxygen-containing CO_2 sources such as flue gas. Another challenge for artificial photosynthesis is the selective synthesis of complex organic molecules.[13−16] Nature transforms CO_2 into a variety of complex molecules using a limited number of biosynthetic intermediates as building blocks.[17] However, in the case of artificial photosynthesis, the selection of such an intermediate is difficult:[3,13,17] ideally, mass transport requires it to be water-soluble, and it should also be easily incorporated into many biosynthetic pathways.[18]

We sought to develop a strategy for artificial photosynthesis, where biocatalysts in their native cellular environments are interfaced directly with semiconductor light-absorbers for unassisted solar CO_2 reduction. Specifically, we envisioned a two-step strategy that mimics natural photosynthesis, where light capture by a biocompatible nanowire array can interface and directly provide reducing equivalents to living organisms for the targeted synthesis of value-added chemical products from CO_2 fixation (Figure 1). Such an integration between

Received: March 31, 2015
Published: April 7, 2015

DOI: 10.1021/acs.nanolett.5b01254
Nano Lett. 2015, 15, 3634−3639

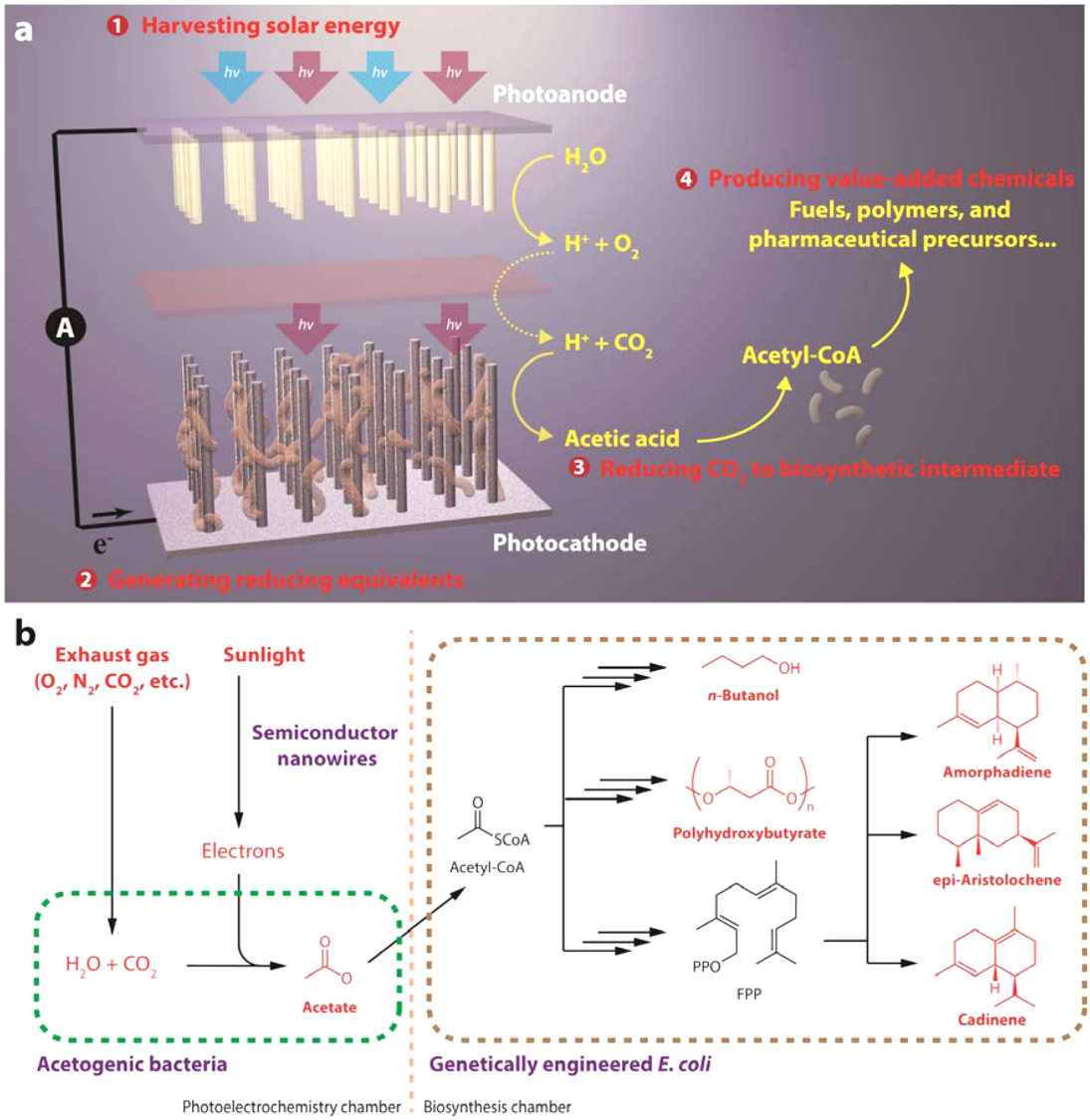

Figure 1. Schematics of a general artificial photosynthetic approach. (a) The proposed approach for solar-powered CO_2 fixation includes four general components: (1) harvesting solar energy, (2) generating reducing equivalents, (3) reducing CO_2 to biosynthetic intermediates, and (4) producing value-added chemicals. An integration of materials science and biology, such an approach combines the advantages of solid-state devices with living organisms. (b) As a proof of concept, we demonstrate that under mild conditions sunlight can provide the energy to directly treat exhaust gas and generate acetate as the biosynthetic intermediate, which is upgraded into liquid fuels, biopolymers, and pharmaceutical precursors. For improved process yield, *S. ovata* and *E. coli* are placed in two separate containers. FPP = farnesyl pyrophosphate.

materials science and biology separates the demanding dual requirements for light-capture efficiency and catalytic activity, respectively, and provides a route to bridge efficient solar conversion in robust solid-state devices with the broad synthetic capabilities of living cells.[10] This artificial photosynthesis strategy is distinct from the active area of microbial electrosynthesis,[19] in that the nanomaterials carry out both light-harvesting and delivery of reducing equivalents. Here, as a first step, we demonstrate a stand-alone, solar-powered system[6,20−24] composed of silicon (Si) and titanium dioxide (TiO_2) nanowire arrays as the light-capturing units[22] to mimic the "Z-scheme"[2,25,26] and *S. ovata* as the cellular catalyst,[27,28] which can effectively reduce CO_2 under mild conditions (e.g., aerobic atmosphere, neutral pH, and temperatures under 30 °C) and produce acetate for up to 200 h under simulated sunlight, with an energy-conversion efficiency of up to 0.38%. Such an system, where CO_2-reducing bacteria are directly interfaced with a photoactive semiconductor, to the best of our knowledge, represents the first example of microbial photoelectrosynthesis, which is different from conventional microbial electrosynthesis wherein microbes do not directly interact with light-absorbing devices.[19,28] The nanowire−bacteria hybrids possess a high reaction rate of CO_2 reduction, and the presence of the nanowire array creates a local anaerobic environment that allows strict anaerobes to continue CO_2 reduction aerobically (21% O_2), which is important for practical application. Finally, the acetate intermediate represents a biosynthetic precursor to a wide variety of potential fine and

DOI: 10.1021/acs.nanolett.5b01254
Nano Lett. 2015, 15, 3634−3639

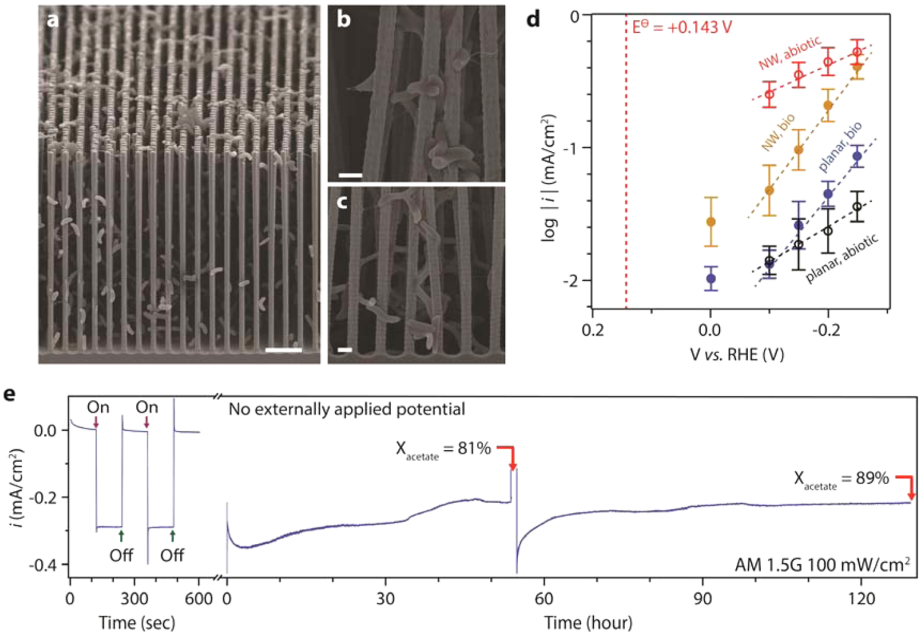

Figure 2. Unassisted solar-powered acetate production from the nanowire–bacteria hybrid device. (a) Cross-sectional SEM image of the three-dimensional network in the nanowire-bacteria hybrid. (b, c) Magnified images at different depths of the nanowire array. (d) Tafel plots, the logarithmic current density versus applied electrochemical voltage, are plotted for different electrode configurations (n = 2). Detailed data are summarized in Supporting Information Figure 2d. Filled blue circle ("planar, bio"), planar electrode loaded with bacteria; filled yellow circle ("NW, bio"), nanowire electrode loaded with bacteria; open black circle ("planar, abiotic"), bare planar electrode; open red circle ("NW, abiotic"), bare nanowire electrode. (e) Measurement of unassisted solar-powered CO_2 reduction for more than 5 days, n = 6. During the experiment the system was purged with 20% CO_2/80% N_2. In the plot $X_{acetate}$ is the product selectivity (Faradaic efficiency) of acetic acid generation. The scale bars are 5 μm (a) and 1 μm (b, c).

commodity chemicals via acetyl coenzyme A (acetyl-CoA), including functionalized aliphatics and aromatics, lipids, alkanes, and complex natural products. By simply selecting specific genetically engineered *E. coli* strains,[18,29−31] our strategy of artificial photosynthesis can be programmed to produce a variety of products with minimal modification, providing a versatile and amenable platform for solar-driven CO_2 reduction to value-added fuels, chemicals, and materials.

The system starts by interfacing light-absorbing Si nanowire arrays with an acetogenic organism, *S. ovata*.[27] Si nanowire arrays capture light for efficient solar energy conversion and provide high surface areas to interface with catalysts.[22,26] The strictly anaerobic homoacetogen *S. ovata* metabolizes CO_2 via the energy-efficient Wood–Ljungdahl pathway and has been reported to accept electrons from graphite electrodes to reduce CO_2 into acetic acid.[28] The integration was realized by directly culturing *S. ovata* within a Si nanowire array passivated by a 30 nm TiO_2 protection layer, using buffered brackish water medium with trace vitamins as the only organic component (see Methods, Supporting Information Figure 1a). After an initial incubation period, a steady-state nanowire–bacteria hybrid structure was formed. In such a structure, the bacteria formed an interconnected network among the nanowires (Figure 2a and Supporting Information Figure 2). Careful characterization with scanning electron microscopy (SEM) indicates that bacteria populate the array quite uniformly without apparent mass transport issues (Figure 2b,c). The cell loading of *S. ovata* within the nanowire array is 4.4 ± 1.0 times of that observed on a planar Si electrode (1.4 ± 0.1 vs 0.32 ± 0.07 cells per geometric μm^2, n = 4) (Supporting Information Figure 2d), revealing increased contact interfaces between bacteria and electrodes in this high-surface-area platform. The proposed half-reaction of CO_2 reduction is

$$2CO_2 + 7H^+ + 8e^- \rightarrow CH_3COO^- + 2H_2O$$

$$E^0 = +0.143 \text{ V vs RHE}$$

From a classic electrochemical analysis without solar illumination (Figure 2d), the nanowire–bacteria hybrids were capable of reducing CO_2 to acetate under continuous sparging with 20% CO_2/80% N_2 with an overpotential η less than 200 mV at 0 V vs reversible hydrogen electrode (RHE) (see Methods), similar as reported in the literature.[28] Additionally the Tafel slope of bacterial catalyzed CO_2 reduction is distinctly different from that of abiotic proton reduction, implying different reaction mechanisms (n = 2). On average, each cell could produce (1.1 ± 0.3) × 10^6 molecules of acetate every second or ca. 10^{12} molecules of acetate over the course of about 5 days at −0.2 V vs RHE (Supporting Information Figure 2c,d), comparable with its intrinsic rate of acetogenic metabolism (Supporting Information Note). Such nano-biohybrids, which operate at ambient temperature, possess a volumetric reaction rate of ca. 2 mol m^{-3} s^{-1}, comparable to the rates in conventional gas phase catalysts (0.1–10 mol m^{-3} s^{-1}) that require much higher temperatures (higher than 100 °C).[32] It also corresponds to ca. 8 electrons s^{-1} nm^{-2} across the semiconductor/electrolyte interface (at −0.2 V vs RHE), suitable to couple with efficient solar devices at 10 mA/cm^2 when integrated into a high-surface-area electrode.[1,6,24,26]

The high reaction rate of the nanowire–bacteria hybrids allows us to construct a solar-powered CO_2-reduction device for the production of acetate as a common biosynthetic

DOI: 10.1021/acs.nanolett.5b01254
Nano Lett. 2015, 15, 3634–3639

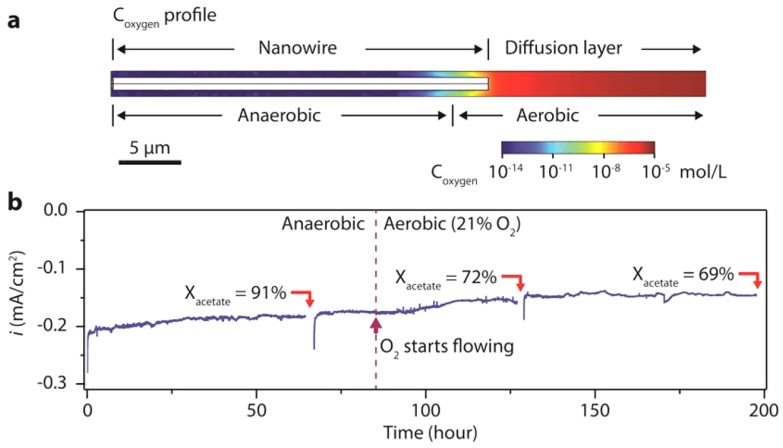

Figure 3. Enhanced oxygen tolerance for nanowire−bacteria hybrids. (a) A numerical simulation illustrates that integrating bacteria into a nanowire array allows for the survival of strict anaerobes in an aerobic environment. The oxygen concentration in the electrolyte decreases logarithmically from the nanowire array's entrance, creating a local anaerobic environment. This is in contrast to the linear decrease of oxygen concentration for a planar electrode (Supporting Information Note and Figure 5). (b) Experimental demonstration of aerobic CO_2 reduction by *S. ovata* when Pt was additionally loaded onto the nanowire electrode, $n = 3$. Constant electrochemical bias (−0.2 V vs RHE) was applied to the Si nanowire electrode, and the current was plotted against time. As highlighted in the plot, the sparging gas of the setup was switched from anaerobic (20% CO_2/80% N_2) to aerobic (21% O_2/10% CO_2/69% N_2) at $t = 85$ h.

feedstock (Figure 1a). Analogous to the two photosystems found in nature,[2,25,26] Si and TiO_2 nanowires were applied as two robust semiconductor light-absorbers to provide the thermodynamic driving force for CO_2 reduction.[22] Specifically, an ion-conductive membrane was placed in between the two electrodes to separate reaction products, and the water-oxidizing TiO_2 nanowire electrode[22] was placed in front of the nanowire−bacteria composite to absorb UV light and prevent possible bacterial photodamage (Figure 1a and Supporting Information Figure 1b). Without any additional energy input, nonzero photocurrent was observed (light chopping experiment in Figure 2e), and CO_2 reduction to acetate was confirmed (see Methods). The overall system produced about 0.3 mA/cm^2 photocurrent under simulated sunlight (AM 1.5G, 100 mW/cm^2) and was stable for more than 120 h (Figure 2e, and the photocathode in Supporting Information Figure 3). Starting from an electrolyte free of organic compounds, acetic acid was steadily produced with a product selectivity (Faradaic efficiency) of 86 ± 9% ($n = 6$) (Figure 2e). The peak photocurrent reached 0.35 mA/cm^2, which corresponds to an energy conversion efficiency of 0.38% for acetic acid production (requires 1.08 V thermodynamically, see Methods). The acetic acid titers were ca. 1.2 g/L (20 mM) within 5 days and could reach over 6 g/L (ca. 100 mM) in M9-MOPS minimal medium (see Methods and Supporting Information Note). In separate control experiments, no acetic acid was detected without incorporation of *S. ovata*, and an isotope-labeling experiment proves that the acetate is produced from CO_2 (Supporting Information Figure 4). These results highlight our ability to upgrade CO_2 to chemicals beyond one-carbon targets. In next-generation designs, we are targeting even higher efficiencies through further improvement on peripheral limitations such as CO_2 mass transport in the electrolyte and the large band gap of the photoanode.[26] Nevertheless, it represents a unique materials−biological hybrid for artificial photosynthesis, which demonstrates unassisted light-driven CO_2 fixation to acetic acid.

An interesting benefit of the nanowire array arises from its selective control of mass transport within the wire assembly.[26,33] Specifically, the design of nanowire−bacteria hybrids allows for the continuation of CO_2 reduction, a reaction catalyzed by strict anaerobe *S. ovata*, under a headspace containing 21% oxygen when an oxygen reduction reaction electrocatalyst (in the current case, Pt, see Methods) was loaded. The similar Tafel slopes of CO_2 reduction for planar and nanowire electrodes (Figure 2d) inform us that mass transport of protons and CO_2 was not a limiting factor within the nanowire array. However, with its limited solubility in water, oxygen can be depleted within the nanowire array logarithmically, distinctly different from a planar counterpart (Supporting Information Note and Figure 5a,b). This arrangement effectively creates a local anaerobic environment at the bottom of the nanowire arrays, as supported by numerical simulation (Figure 3a and Supporting Information Figure 5c). Experimentally, after *S. ovata* had colonized the electrode anaerobically, we switched to an aerobic gas environment with 21% oxygen partial pressure (21% O_2/10% CO_2/69% N_2) (see Methods). Only the nanowire array loaded with Pt maintained its ability to reduce CO_2 and consistently produce acetic acid with a Faradaic efficiency of about 70% ($t = 85$ h, Figure 3b). Compared to the data obtained under anaerobic conditions (20% CO_2/80% N_2), the loss of Faradaic efficiency observed under aerobic conditions (~15%) is related to the oxygen reduction reaction (Supporting Information Figure 6), which can be greatly minimized with improved design of the nanowire−bacteria hybrids (Supporting Information Note). In general, our observation implies that (1) in our system most, if not all, of the acetate is produced from bacteria interfacing directly with nanowires and (2) combining nanowire arrays with CO_2-reducing microorganisms can allow anaerobes to be used in a wider range of applications, such as CO_2 scrubbing from exhaust gas or even open air operation.

Taking advantage of the power of synthetic biology,[18] a wide spectrum of complex organic molecules was synthesized by directly using the solar-derived acetate from oxygen-containing CO_2 feedstock. Under aerobic or microaerobic conditions, genetically engineered *E. coli* can activate acetate into the common biochemical intermediate acetyl-CoA, which then will

DOI: 10.1021/acs.nanolett.5b01254
Nano Lett. 2015, 15, 3634−3639

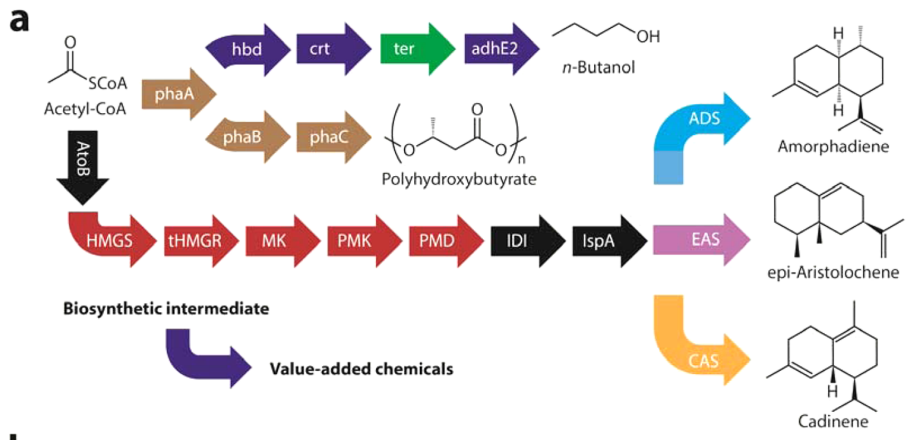

b **Biocatalytic production using genetically engineered *E. coli***

Product	Plasmids	$X_{product}$ (100%)	Titer (mg/L)
n-Butanol	pBT33-Bu2, pCWori-ter.adhE2, pBBR1-MCS2-pTrc-ACS*	25.6±2.1	198±22
Amorphadiene	pAM45, pADS	25.1±2.8	124±10
epi-Aristolochene	pAM45, pEAS	10.6±2.3	39±8
Cadinene	pAM45, pCAS	4.7±1.6	22±7
Polyhydroxybutyrate	pBT33-phaA.phaB.phaC, pBBR1-MCS2-pTrc-ACS*	51.8±8.6	490±177

Figure 4. Biocatalytic production of diverse organic compounds using genetically engineered *E. coli*. (a) Synthetic pathways for the production of a variety of value-added chemicals. Here the names of proteins are listed, and the colors differentiate their genetic origins. In addition to these described pathways, some of the acetyl-CoA are expected to be diverted into the TCA cycle for redox balancing. (b) Solar-derived acetic acid from nanowire−bacteria hybrids was used as the feedstock to yield a variety of chemicals in M9-MOPS medium (t = 5 days). No organic substrates were provided except the solar-derived acetic acid, and the acetate-containing medium solution was produced under aerobic conditions (21% O_2/10% CO_2/69% N_2) using simulated sunlight. Here $X_{product}$ is acetate-to-product conversion efficiency. n = 3 for all reported values. Blue, *Clostridium acetobutylicum*; green, *Treponema denticola*; brown, *Ralstonia eutropha*; black, *E. coli*; red, *Saccharomyces cerevisiae*; light blue, *Artemisia annua*; purple, *Nicotiana tabacum*; yellow, *Gossypium arboreum*. phaA, acetoacetyl-CoA thiolase/synthase; hbd, phaB, 3-hydroxybutyryl-CoA dehydrogenase; crt, crotonase; ter, *trans*-enoyl-CoA reductase; adhE2, bifunctional butyraldehyde and butanol dehydrogenase; phaC, PHA synthase; AtoB, acetyl-CoA acetyltransferase; HMGS, hydroxymethylglutaryl-CoA synthase; tHMGR, truncated hydroxymethylglutaryl-CoA reductase; MK, mevalonate kinase; PMK, phosphomevalonate kinase; PMD, phosphomevalonate decarboxylase; IDI, isopentenyl diphosphate-isomerase; IspA, farnesyl diphosphate synthase; ADS, amorphadiene synthase; EAS, epi-aristolochene cyclase; CAS, cadinene synthase.

be used for the biosynthesis of a variety of complex molecules (Figure 4a). In principle, the acetate-consuming *E. coli* and the solar-powered CO_2-reducing nano-biohybrids can be positioned in a single aerobic reactor. However, for optimized yield these two processes are conducted in separate containers (Supporting Information Note). Here, as a proof of concept, the production of *n*-butanol,[29] PHB biopolymer,[31] and three isoprenoid compounds[30] is demonstrated with H_2O and CO_2 as the starting materials and sunlight as the energy source (Figure 1b and Supporting Information Figures 7 and 8; see Methods). After the solar-powered acetate-production step, the accumulation of the target molecules is correlated with the consumption of acetate (n = 3, Supporting Information Figure 9a), implying the conversion of acetate into the desired products. The yield of target molecules was as high as 26% for *n*-butanol, 25% for one of the isoprenoid compounds (amorphadiene), and up to 52% for PHB biopolymer (Figure 4b and Supporting Information Figure 9b), comparable with literature values.[29−31] Taking into account the 0.38% efficiency from CO_2 to acetic acid, a solar energy-conversion efficiency of 0.20% is achieved from CO_2 to PHB biopolymer, a renewable and biodegradable plastic. Overall, the production of different organic products with vastly different synthetic pathways (Supporting Information Figure 7) proves the versatility of the integrated approach starting from one common biochemical building block, analogous to natural photosynthesis.

The results reported here outline a solar-energy conversion process that combines the strengths of semiconductor nanodevices and bacterium-based biocatalysts (Figure 1a). Key advantages of the nanowire-based device are the enhanced oxygen tolerance that allows exhaust gas to be directly fed into the system, thereby enabling use of strict anaerobes with aerobes, as well as the high measured CO_2 fixation activity of the nanowire−bacteria hybrid. Moreover, this modular platform simplifies the overall system design by allowing for the production of a variety of molecular targets, without any setup change in the components for light capture and CO_2 reduction into acetate, by varying only the downstream microorganisms.

DOI: 10.1021/acs.nanolett.5b01254
Nano Lett. 2015, 15, 3634−3639

■ ASSOCIATED CONTENT

Supporting Information

Methods; additional discussion; Figures 1−10. This material is available free of charge via the Internet at http://pubs.acs.org.

■ AUTHOR INFORMATION

Corresponding Authors

*E-mail p_yang@berkeley.edu (P.Y.).
*E-mail mcchang@berkeley.edu (M.C.Y.C.).
*E-mail chrischang@berkeley.edu (C.J.C.).

Author Contributions

C.L. and J.J.G. contributed equally for this work.

Notes

The authors declare no competing financial interest.

■ ACKNOWLEDGMENTS

We thank Dr. Miao Wen for use of the ACS and PHB plasmids. We also acknowledge Yude Su, Dr. Jongwoo Lim, and Dr. Sarah F. Brittman for helpful discussions. P.Y. thanks support from DOE/LBNL DE-AC02-05CH11231 (PChem, P.Y.). C.J.C. and M.C.Y.C. thank support from DOE/LBNL DE-AC02-05CH11231, FWP no. CH030201 (C.J.C. and M.C.Y.C.). C.J.C. is an Investigator with the Howard Hughes Medical Institute. J.J.G., K.K.S., and E.M.N. acknowledge the NSF-GRFP for funding. J.J.G. also thanks NIH Training Grant 1 T32 GMO66698 for support.

■ REFERENCES

(1) Lewis, N. S.; Nocera, D. G. *Proc. Natl. Acad. Sci. U. S. A.* **2006**, *103*, 15729−15735.
(2) Barber, J. *Chem. Soc. Rev.* **2009**, *38*, 185.
(3) Concepcion, J. J.; House, R. L.; Papanikolas, J. M.; Meyer, T. J. *Proc. Natl. Acad. Sci. U. S. A.* **2012**, *109*, 15560−15564.
(4) Magnuson, A.; et al. *Acc. Chem. Res.* **2009**, *42*, 1899−1909.
(5) Gust, D.; Moore, T. A.; Moore, A. L. *Acc. Chem. Res.* **2009**, *42*, 1890−1898.
(6) Luo, J.; et al. *Science* **2014**, *345*, 1593−1596.
(7) Zhao, Y.; et al. *Proc. Natl. Acad. Sci. U. S. A.* **2012**, *109*, 15612−15616.
(8) Tachibana, Y.; Vayssieres, L.; Durrant, J. R. *Nat. Photonics* **2012**, *6*, 511−518.
(9) Gray, H. B. *Nat. Chem.* **2009**, *1*, 7.
(10) Blankenship, R. E.; et al. *Science* **2011**, *332*, 805−809.
(11) Reda, T.; Plugge, C. M.; Abram, N. J.; Hirst, J. *Proc. Natl. Acad. Sci. U. S. A.* **2008**, *105*, 10654−10658.
(12) Bachmeier, A.; Hall, S.; Ragsdale, S. W.; Armstrong, F. A. *J. Am. Chem. Soc.* **2014**, *136*, 13518−13521.
(13) Appel, A. M.; et al. *Chem. Rev.* **2013**, *113*, 6621−6658.
(14) Kumar, B.; et al. *Annu. Rev. Phys. Chem.* **2012**, *63*, 541−569.
(15) Barton, E. E.; Rampulla, D. M.; Bocarsly, A. B. *J. Am. Chem. Soc.* **2008**, *130*, 6342−6344.
(16) Li, C. W.; Ciston, J.; Kanan, M. W. *Nature* **2014**, *508*, 504−507.
(17) Li, H.; Liao, J. C. *Energy Environ. Sci.* **2013**, *6*, 2892−2899.
(18) Keasling, J. D. *Science* **2010**, *330*, 1355−1358.
(19) Lovley, D. R.; Nevin, K. P. *Curr. Opin. Biotechnol.* **2013**, *24*, 385−390.
(20) Khaselev, O. A.; Turner, J. A. *Science* **1998**, *280*, 425−427.
(21) Brillet, J.; et al. *Nat. Photonics* **2012**, *6*, 824−828.
(22) Liu, C.; Tang, J.; Chen, H. M.; Liu, B.; Yang, P. *Nano Lett.* **2013**, *13*, 2989−2992.
(23) Reece, S. Y.; et al. *Science* **2011**, *334*, 645−648.
(24) Cox, C. R.; Lee, J. Z.; Nocera, D. G.; Buonassisi, T. *Proc. Natl. Acad. Sci. U. S. A.* **2014**, *111*, 14057−14061.
(25) Nozik, A. J. *Appl. Phys. Lett.* **1976**, *29*, 150−153.
(26) Liu, C.; Dasgupta, N. P.; Yang, P. *Chem. Mater.* **2013**, *26*, 415−422.
(27) Möller, B.; Oβmer, R.; Howard, B.; Gottschalk, G.; Hippe, H. *Arch. Microbiol.* **1984**, *139*, 388−396.
(28) Nevin, K. P.; Woodard, T. L.; Franks, A. E.; Summers, Z. M.; Lovley, D. R. *mBio* **2010**, *1*, e00103−10.
(29) Bond-Watts, B. B.; Bellerose, R. J.; Chang, M. C. Y. *Nat. Chem. Biol.* **2011**, *7*, 222−227.
(30) Chang, M. C. Y.; Eachus, R. A.; Trieu, W.; Ro, D.-K.; Keasling, J. D. *Nat. Chem. Biol.* **2007**, *3*, 274−277.
(31) Sim, S. J.; et al. *Nat. Biotechnol.* **1997**, *15*, 63−67.
(32) Levenspiel, O. *Chemical Reaction Engineering*, 3rd ed.; John Wiley & Sons: New York, 1999; p 5.
(33) Xiang, C.; Meng, A. C.; Lewis, N. S. *Proc. Nat. Acad. Sci. U. S. A.* **2012**, *109*, 15622−15627.

DOI: 10.1021/acs.nanolett.5b01254
Nano Lett. 2015, 15, 3634−3639